CHAPTER V

INSTRUMENTATION, CALIBRATION AND EXPERIMENTAL PROCEDURE

5.1 INTRODUCTION

To prove the proposed theoretical model for the traction performance of the tracked vehicle on soft terrain surface based on the analytical method, *in situ* soil characterization was necessary. In this research project, the bevameter technique was used to acquire soil characteristics for shear strength, rubber-soil friction as well as the pressure-sinkage relationship.

For validation of the predicted results, a series of full-scale drawbar pull tests were conducted in the field. The parameters measured during the drawbar pull test included the drawbar pull, the torque to one side drive shaft of the tractor and the theoretical and actual travel speeds was based on which the total slippage was calculated. The slip between wheel and track measured manually by means of marks on the wheel and the track to derive the difference between the calculated wheel travel distances to the measured track travel distance after a certain number of revolutions of the wheel.

The contact and the tangential forces on the ground contact surface between a track element and the soil were also measured by using two small specially designed extended octagonal ring transducers, mounted on the track basis. From the measured contact force, the distribution of the contact pressure along the track was derived. The total tangential tractive effort was calculated based on the summation of the measured tangential forces.

All the experimental work was conducted under field conditions at the Experimental Farm, University of Pretoria. To identify the influence of the soil water content on drawbar performance it was decided to perform the tests under three different values of soil water content, controlled by irrigating the test site several days before a test. In order to achieve realistic test conditions as expected, the field was carefully chosen and disk ploughed. The tests were also conducted during the dry winter season to eliminate the influence of rainfall.

A computerized data acquisition and logging system was built and used to pre-process and record all the data concerned.

5.2 APPARATUS FOR SOIL CHARACTERIZATION

To obtain the soil parameters necessary for the traction modelling based on the analytical methods, an instrumented apparatus applying the bevameter technique was built in the Department of Agricultural Engineering, University of Pretoria (Yu, 1996). This linear shear and soil sinkage apparatus was similar to the one originally developed at the University of California, Davis Campus (Upadhyaya et al, 1993).

The instrumented apparatus as shown in Figure 5.1, can be used to measure:

- linear soil shear and frictional characteristics for steel-soil and rubber-soil contact respectively;
- soil contact pressure-sinkage parameters; and
- soil cone index.

The main frame (M) was carried by a front mounted tractor three point linkage (L).

A double acting hydraulic cylinder and set of loading blade springs (B) applied a predetermined constant vertical load to the main frame (M) and adjustable feet (A).

The grouser carrier frame (F) was moved horizontally by a hydraulic cylinder (H_2) supported by two horizontal brass bearings sliding over round stainless steel rod slides (S_2). To accommodate slip sinkage during the test the anchor of the traction cylinder (H_2) slides vertically on a brass bush and rod (S_3). To ensure minimal frictional influence on the horizontal shear force, measured by the load cell between the grouser carrier frame and piston assembly (H_2), the grouser was carried by four identical vertical adjustable arms (L_1) with ball joints.

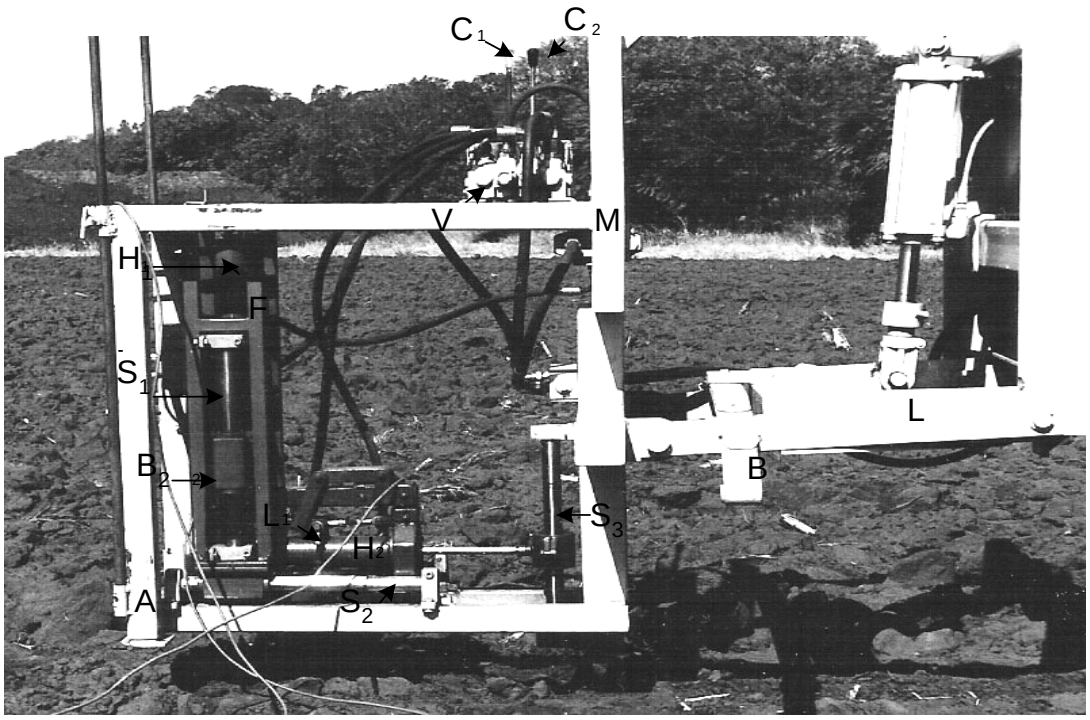

A – adjustable feet	B – loading blade springs	B_2 – moving blocks
C_1 – control lever	C_2 – second control lever	F – carrier frame
H_1 – vertical cylinder	H_2 – piston assembly	L – three point linkage
M – main frame	S_1 – vertical piston rod	S_2 – rod slides
S_3 – brass bush and rod	V – pressure control valve	

Figure 5.1. Linear shear meter used for soil shear, soil-rubber friction as well as sinkage characterization.

Two separate hydraulic circuits were used to prevent interaction between the vertical and horizontal loading. The vertical force was applied by a pump and circuit, with a hydraulic cylinder between the main frame (M) and unit with two parallel moving blocks (B_2). The vertical load cell was mounted between (B_2) and the grouser carrier.

The applied vertical force was kept constant during slip sinkage by supplying surplus oil and using a special adjustable pressure control valve (V). During the test the vertical load was applied with the supply control lever (C_1) fully open and the control valve (V) set at a specific release pressure, with the surplus oil flowing back to the tank.

The second control lever (C_2) activated the second hydraulic circuit and supplied oil to the horizontal cylinder (H_2) whilst the vertical hydraulic cylinder (H_1) followed the slip sinkage action and applied a constant vertical load. The vertical and horizontal displacement of the grouser was recorded via two rotational potentiometers with woven string and a rotary spring for automatic return.

Two industrial S-type weighing scale load cells were used to measure the applied vertical and horizontal loads independently. The shear grousers, sinkage plates and cone penetrometer with different shapes, dimensions, and surface materials could easily be removed and replaced when necessary.

The analog signals from the load cells and the potentiometers had to be pre-processed by an A/D converter before being recorded by the data acquisition system.

Three sinkage steel plates with different dimensions were used to characterize the soil pressure-sinkage relationships. Two different steel shear grousers were used to obtain the soil shear characteristics, whilst a standard rubber-covered track element was used to measure the rubber-soil frictional characteristics.

Figure 5.2 shows the grouser shear plates, the sinkage plates, the track element and the cone penetrometer used for soil characterization with the instrumented bevameter.

The dimensions of the shear grousers and the sinkage plates are shown in Table 5.1 and Table 5.2 respectively.

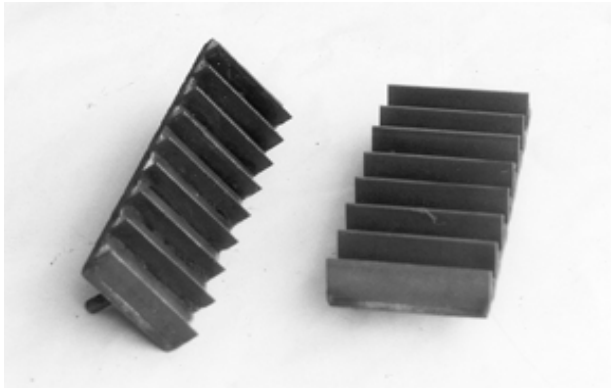

(a) shear grousers

(b) sinkage plates

(c) track element

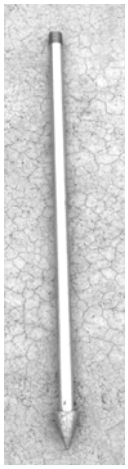

(d) cone penetrometer

Figure 5.2. Components used for soil characterization.

Table 5.1. Dimensions of the rectangular steel shear grousers and the rubber track element.

Dimension	Length, mm	Width, mm	Grouser height, mm
Steel shear grouser	240	60	10
Steel shear grouser	220	80	12
Rubber track element	500	70	Smooth rubber surface

Table 5.2. Dimensions of the steel sinkage plates.

Sinkage plate	Width, mm	Length, mm	Aspect ratio (L/W)
No. 1	70	210	3
No. 2	60	240	4
No. 3	55	285	5.18

5.3 THE EXTENDED OCTAGONAL RING TRANSDUCERS FOR MEASURING THE DISTRIBUTION OF CONTACT PRESSURE AND TANGENTIAL STRESS

5.3.1 Design of the transducer

Two identical extended octagonal ring transducers were built in order to measure the distribution of contact pressure and tangential stresses.

The basic shape and dimensions of the octagonal ring transducer are shown in Figure 5.3.

The values of L_o and r_o were chosen to accommodate the limited space available between the track element and the base plate over the track cable assembly. The value of b was chosen to provide for sufficient supporting area and stiffness to mount the transducer onto the track. The transducers were machined from a solid block of EN24 alloy steel, and heat-treated for an ultimate tensile strength of about 1500MN/m^2 on which the preliminary design was based. Both high sensitivity and sufficient stiffness within the elastic deformation range was necessary. By applying the equations as reviewed in Chapter 2, the thickness t_o, at the middle point of the flat surface was initially calculated as 1.9mm. The vertical force was accepted as 2000N with an allowable working stress of 750MN/m^2. For machining purpose, the value of

t_o was eventually adjusted to 2mm. The dimensions for the two transducers are shown in Table 5.3.

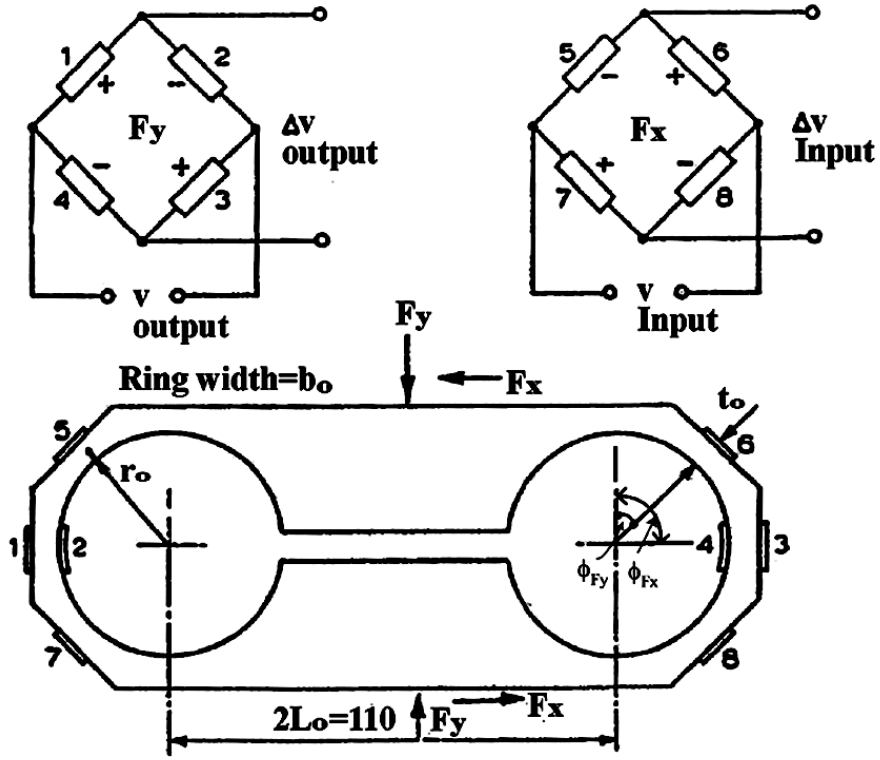

Figure 5.3. Design parameters and forces for the extended octagonal ring transducer.

Table 5.3. The dimensions of the octagonal ring transducers.

r_o, mm	L_o, mm	t_o, mm	b_o, mm	ϕ_{Fx}, deg	ϕ_{Fy}, deg
16	55	2	20	90	45

The nodal angle for force F_x was determined as 90° by trial and error fixing of the strain gauges at different angles with the least interference on force F_x by force F_y and vice versa,. For force F_y, the nodal angle was identified as 45°.

The ratio of r_o/t_o=8 is larger than 5 and is sufficiently large for thin ring theory to be accepted as valid on which the design was based (Godwin, 1975).

5.3.2 Calibration and installation of the transducers

For each extended octagonal ring transducer, eight 120Ω strain gauges were used to form two Wheatstone bridges. After the strain gauges were fixed and the circuits connected, the two transducers were calibrated using a special frame on which the horizontal and the vertical loads were applied independently. The excitation voltage to the bridges was 5 volt and the outputs for calibration were measured with a Hewlett-Packard high-sensitivity multi-meter.

The preliminary calibrations showed some unacceptably high cross sensitivity errors for the bridge measuring force F_y caused by force F_x (Yu & du Plessis, 1996). Further investigation and modifications were undertaken to correct the error by inserting two thicker steel spacers (B in Figure 5.4) on both mounting surfaces of the transducer to ensure that the elastic deformation of the transducer was not interfered with by improper constraints as shown in Figure 5.4.

Prior to the field tests, the two transducers were finally calibrated to obtain the results as shown in Figures 5.5 to 5.8. The regression data proved that the outputs for both transducers were highly linear with the correlation coefficients ≥ 0.998 over the full load range tested. The recorded cross sensitivity error for the two transducers was less than 2%. The line is shown at the bottom of each graph. The calibration results are shown in Table 5.4.

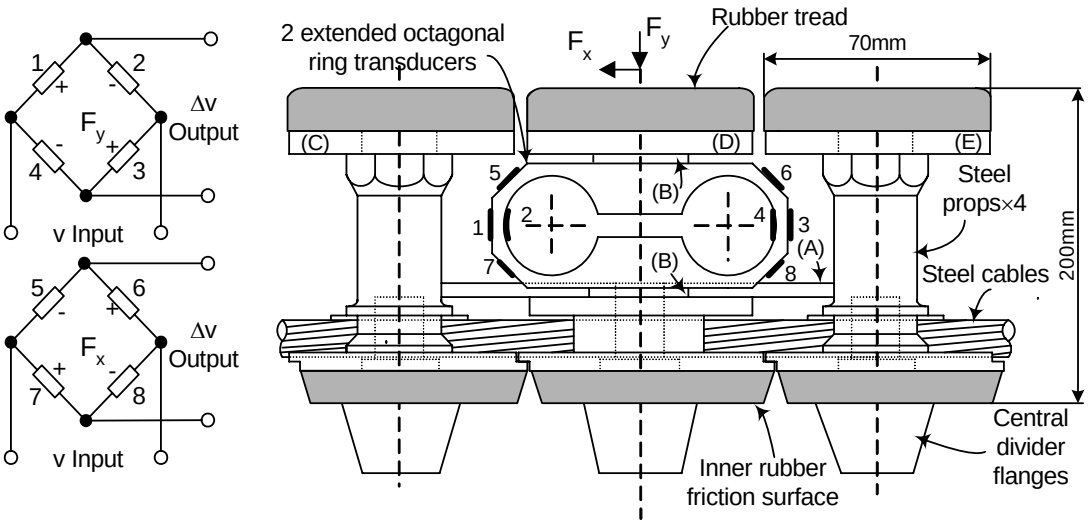

Figure 5.4. The installation of the octagonal ring transducers on the track element.

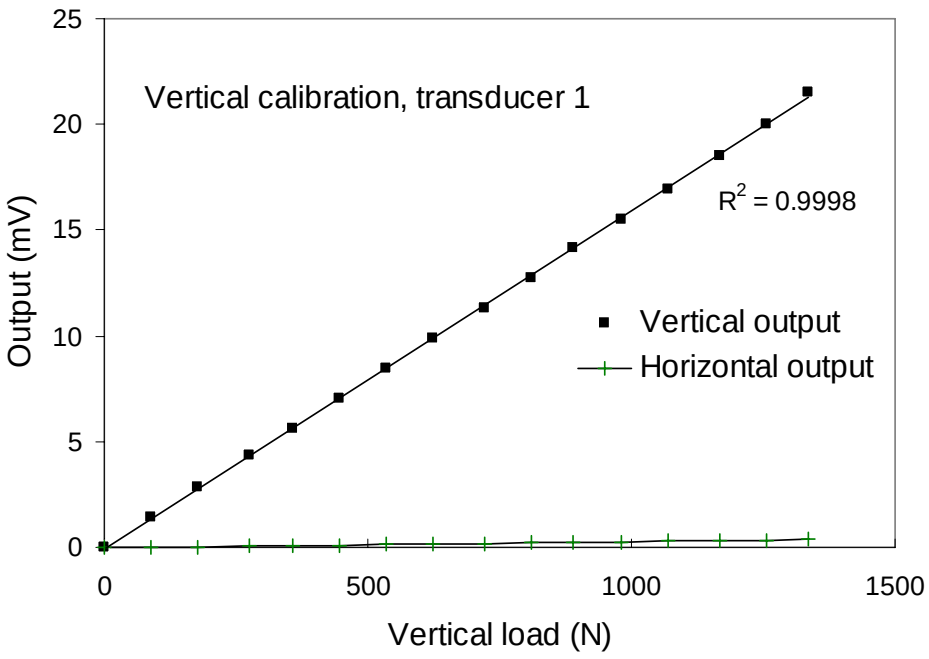

Figure 5.5. Vertical calibration of the octagonal ring transducer 1.

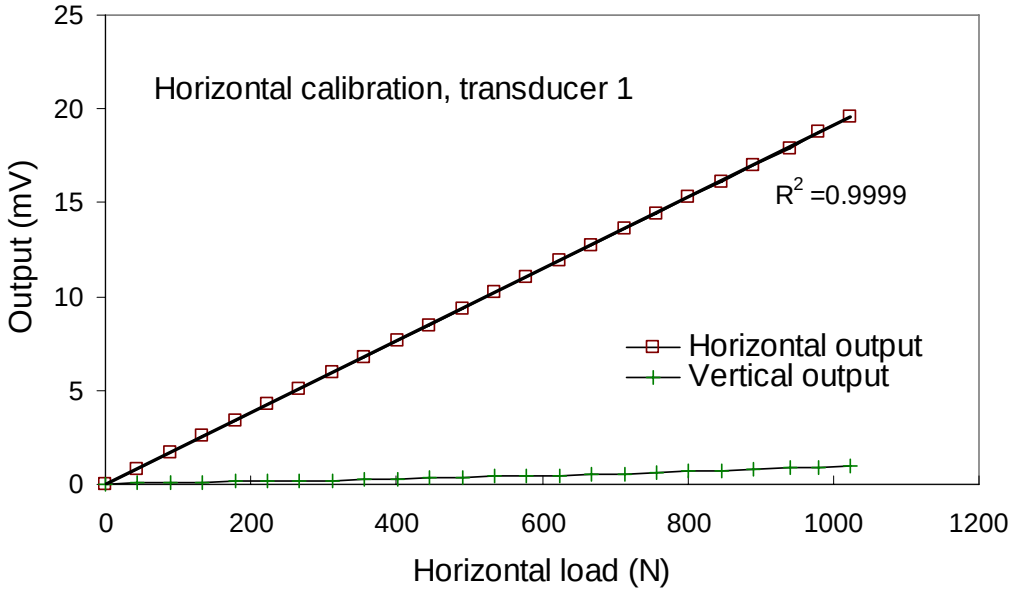

Figure 5.6. Horizontal calibration of the octagonal ring transducer 1.

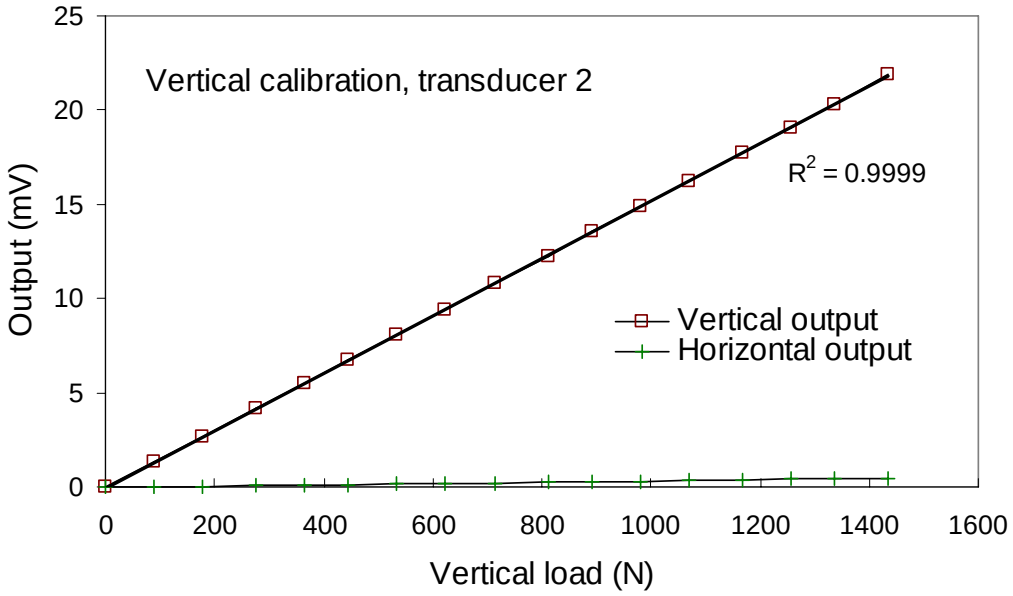

Figure 5.7. Vertical calibration of the octagonal ring transducer 2.

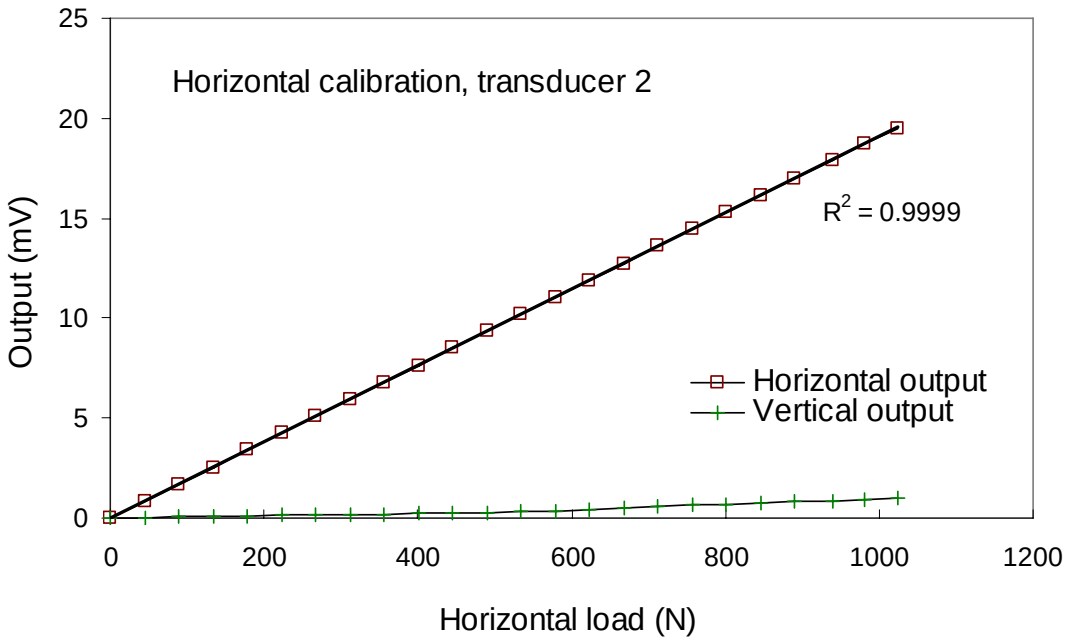

Figure 5.8. Horizontal calibration of the octagonal ring transducer 2.

Table 5.4. Calibration results for the two octagonal ring transducers.

	Transducer 1		Transducer 2	
	Vertical load F_V	Horizontal load F_H	Vertical load F_V	Horizontal load F_H
Sensitivity (mV/N·V)	0.62180	0.52453	0.65049	0.52534
Correlation coefficient	0.99981	0.99991	0.99995	0.99992

The two extended octagonal ring transducers were fitted between the track base assembly and the track element as shown in Figure 5.9 and Figure 5.10. Two steel plates (A) were inserted between the columns of the adjacent track elements to prevent them from touching the middle one onto which the transducers were mounted. In this way the tangential stress could be measured without interference from the neighboring track elements (Figures 5.9 and 5.10). By mounting the two transducers side by side along the width of the track, the total force on the track element could be measured by adding the outputs from the two transducers in vertical and tangential directions respectively. Accordingly, the contact pressure and the shear-friction stress could be calculated by dividing the corresponding load by the contact area.

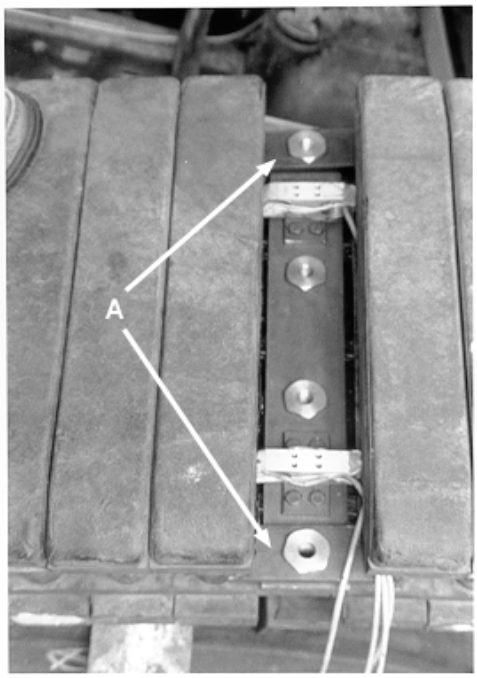

Figure 5.9. Top view of the two transducers installed side by side on the track.

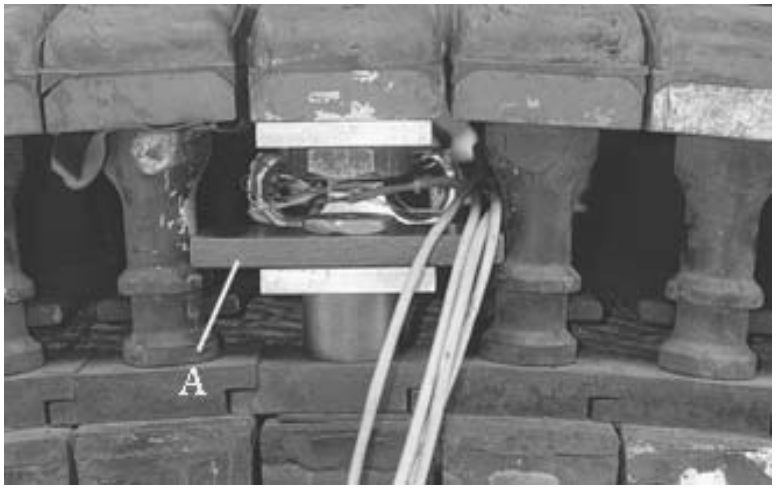

Figure 5.10. Side view of the two octagonal ring transducers installed between the track element and the track base assembly.

5.4 INSTRUMENTATION FOR MEASURING TORQUE, SLIP AND DRAWBAR PULL

5.4.1 Instrumentation for measuring the side shaft torque

By using a special differential system in the tractor drive train, the torque is equally divided between the two side shafts under normal operational conditions. The drive torque and speed are also equally split to the two side shafts for straight line traveling. To simplify the instrumentation for measurement, it was decided to measure the torque and the speed for only one side shaft as torque was equally split between the two side shafts by the interlinked differential.

Wire-type strain gauges were chosen to measure the side shaft torque and the circuit was connected into Wheatstone bridges (Figure 5.11). To reduce the noise errors during the signal transfer, the output signal for the torque was firstly amplified and conditioned by a circuit fixed to the rotating shaft. The amplified signal was transmitted via a slip ring and a cable system to the data acquisition system. The torque transducer was calibrated prior to the re-assembly of the drive axle by using a

three meter long steel arm fixed to the drive shaft and step by step loading it by standard weights. The calibration data for the torque transducer is shown in Figure 5.12.

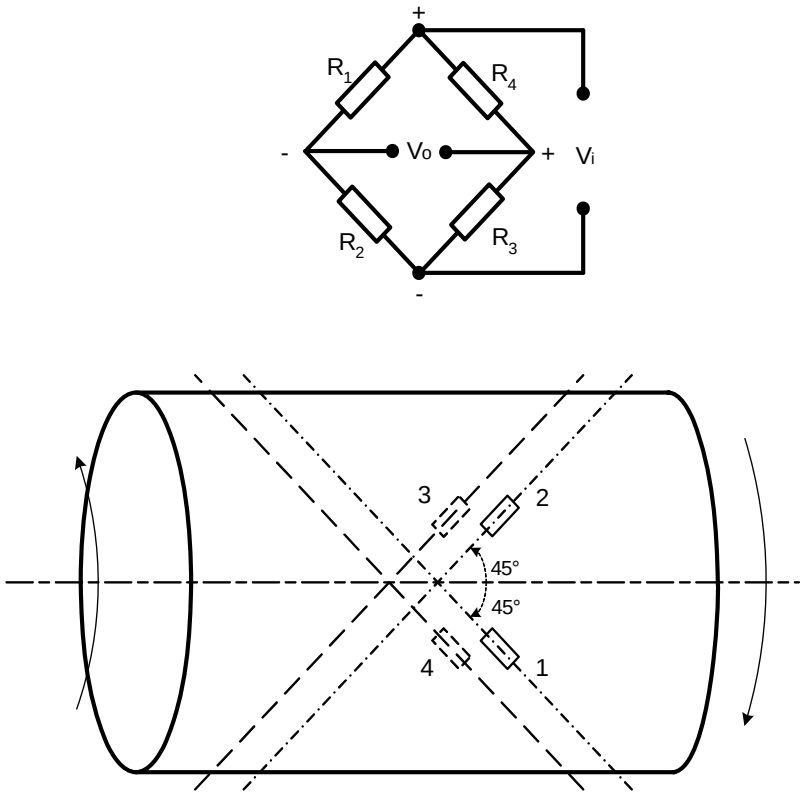

Figure 5.11. The strain gauges and the circuit to measure the side shaft torque.

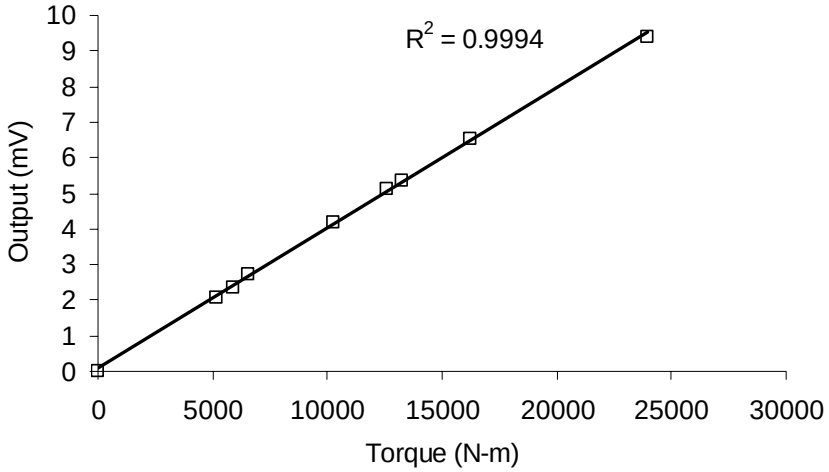

Figure 5.12. The calibration results for the torque transducer.

5.4.2 Instrumentation for measuring speed and slip

Two speed sensors using photoelectric counters were built to measure the speeds (Figure 5.13). The sensor consisted of a circular and thin transparent plastic disk with uniformly distributed radial black printed stripes at the outer edge (Figure 5.13, A) housed in a circular aluminum housing (B) and a micro optical emitting switch (C) on the side of the box. The optical switch sensed the number of the radial black stripes passing the slot which were subsequently recorded as a frequency signal by a special pulse counter circuit.

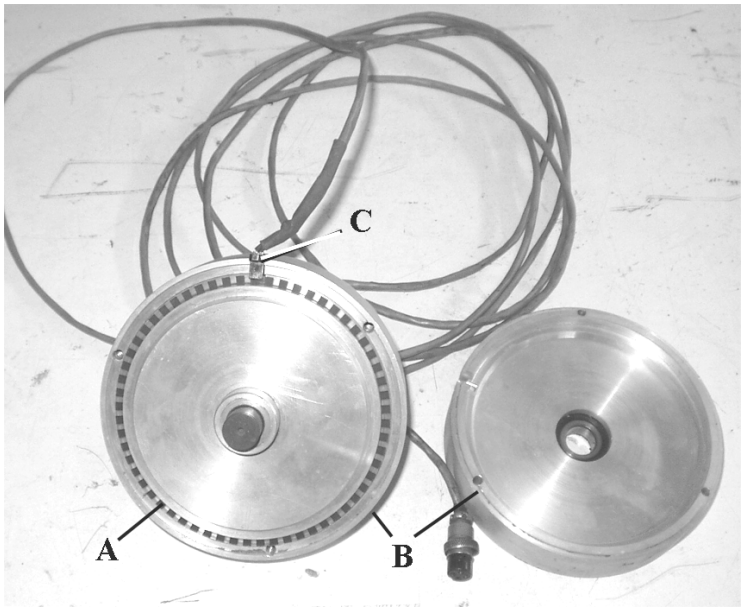

Figure 5.13. Construction of the speed transducers.

Figure 5.14 shows the two instrumented speed transducers mounted on the side shaft of the tractor.

The frequency signals from the speed transducers and the analog signals from the torque transducer on the side shaft were transferred via a slip ring unit (A) with special carbon brushes (Figure 5.14). The rotational speed of the rear side shaft was recorded by the speed transducer unit (B). The true ground speed was recorded by

the speed transducer unit (D) fixed to a drum driven by a cable and anchored to the soil surface. The cable was rewound by winch (C) and braked by (E) to prevent the cable from overrunning. Wheel (F) was used for changing the cable direction.

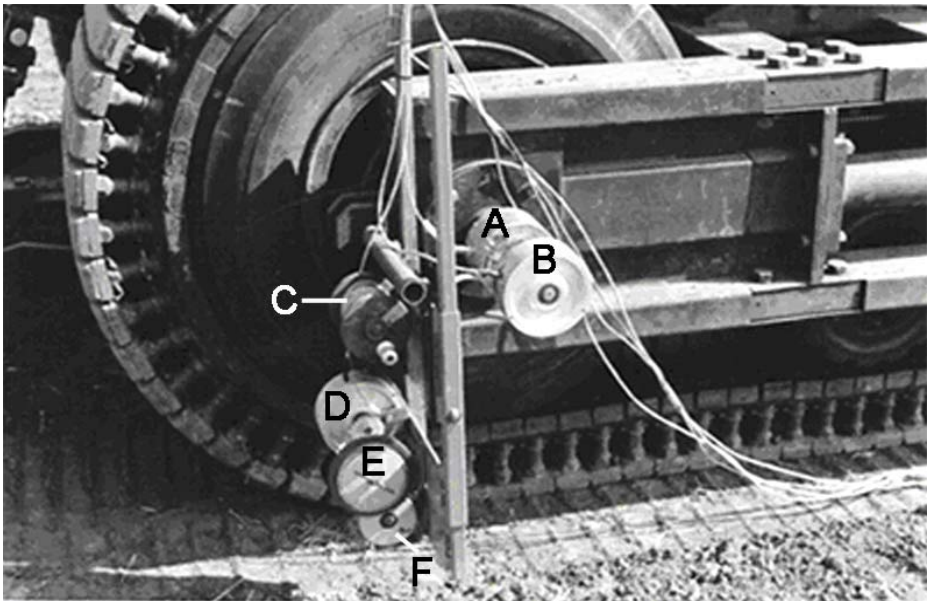

A - slip ring
B – speed transducer unit for theoretical speed
C – winch
D – speed transducer unit for actual speed
E – winch brake

Figure 5.14. The speed transducers, the brush and rotational slip ring unit mounted on the side shaft of the tractor.

The total slip of the track S_t, including wheel to track slip, was obtained by measuring the theoretical speed V_t and the ground speed V of the tractor.

$$S_t = \frac{V_t - V}{V_t} \times 100\% \tag{5.1}$$

The angular speed ω of the shaft of the aluminum unit was obtained based on the frequency of the speed pickup by applying equation (5.2):

$$\omega = 2\pi f / n \tag{5.2}$$

Where n is the total number of the black stripes for 360 degree engraved circle on the plastic sheet.

One of the two aluminum counter units was directly mounted on the extended part of the side drive shaft (Figure 5.13 (A)) and was used to measure the theoretical speed V_t as:

$$\begin{aligned} V_t &= 2\pi r_t \omega_t \\ &= 4\pi^2 r_t f_t \\ &= C_t f_t \end{aligned} \tag{5.3}$$

Where

r_t = the rolling radius of the track, (m).

ω_t = the theoretical angular speed, (rad/s).

f_t = the frequency recorded up by the theoretical speed sensor.

C_t = a constant.

The travel distance for a specified number of revolutions of the drive wheel N_t was measured when the crawler tractor was propelled by its own engine but with zero drawbar pull on concrete road surface. Then the travel distance for the same specified number of revolutions of the drive wheel N_t was measured again when the crawler tractor in neutral gear was towed by another tractor. The rolling radius of the track was calculated based on applying the average travel distance L_t from the above two runs.

Thus,

$$r_t = \frac{L_t}{2\pi N_t} \tag{5.4}$$

The effective radius of the drum was determined by taking the effect of cable diameter into account. When the drum was driven by cable winding over it, the revolutions of the drum N_d were counted and the corresponding travel distance of the cable L_d measured. The effective radius of the drum was therefore calculated by:

$$r_d = \frac{L_d}{2\pi N_d} \tag{5.5}$$

Similarly, the ground travel speed V can then be obtained as:

$$\begin{aligned} V &= 2\pi r_d \omega_d \\ &= 4\pi^2 r_d f_a \\ &= C_a f_a \end{aligned} \tag{5.6}$$

Where

r_d = effective radius of the drum, (m).

ω_d = angular speed of the pulley, (rad/s).

f_a = the frequency recorded by the actual speed sensor.

C_a = a constant to calculate the theoretical speed related to r_d and π.

For the above instrumented device, the recorded slip was the total slip including the wheel-track slip and the track-soil slip.

The wheel-track slip was measured for the field tests by manually marking the tyre surface and the track element. The first marks were made on the tyre and the specified track element at the same time. After several revolutions, the travel distances of the marked point on the tyre and the marked track element were measured and compared to obtain the difference between the two. Then the slip between the wheel and the track was determined.

5.4.3 Instrumentation for measuring drawbar pull

The drawbar pull was measured by mounting a 10 ton industrial load cell, from a local supplier, namely Load Cell Services, between the tested crawler tractor and one or two loading wheeled tractors in series as shown in Figure 5.15. To ensure that the effective drawbar pull was measured, the hitch points of the towing bars for the tractors were adjusted to be parallel to the ground surface.

The analog signal from the load cell was transmitted to the A/D card signal amplifier and conditioner and the data logging system via a cable.

Figure 5.15. The tractors in series for the drawbar pull tests.

5.5 THE COMPUTERIZED DATA LOGGING SYSTEM

All measured analog and digital signals for the field experiments were recorded by an IBM PC compatible computer via a PC30 A/D converter card.

The analog signals, e.g. the signals from the force transducers and octagonal ring transducers, were pre-processed or conditioned before data logging. A signal conditioner mainly composed of 1A31B IC chips from Analog Devices and other associated components were used for amplification and conditioning the signals. The analog signals were then amplified to a specified range for the PC30 card and the noise was filtered. By applying a specially designed circuit to accommodate the 1A31B IC chips, the excitation voltages to the analog transducers and to the frequency and digital transducers were adjustable to suit the display and recording range of the data logging system. As a routine task, the final signals to be recorded

by the PC based data logging system were observed and calibrated before each field test.

The only exception was the analog signal from the side shaft torque transducer which was pre-processed by another amplifying circuit, mounted inside the hub of the drive wheel. An instrumentation amplifier AD620 supplied by Analog Devices was used for the torque signal because of its compact size. By using a slip ring assembly, the amplified signal from the torque transducer was transferred from the rotating side shaft directly to the PC30 card.

In the computer, Stat30 and Waveview software were used to record the data from all the channels. The basic functions of the software included the pre-set and adjustment for sampling frequencies, recording time, offset of signals, channels for data recording, magnitude range of signals and other parameters. The recording of the data was triggered by one touch of the keyboard. The software was also capable of recording data in several specific formats including special graphic format, numeric format and plain text format for further processing with spread sheets or other software.

The flow chart for data processing and recording is shown in Figure 5.16. Figure 5.17 shows the hardware housed in the tractor cab.

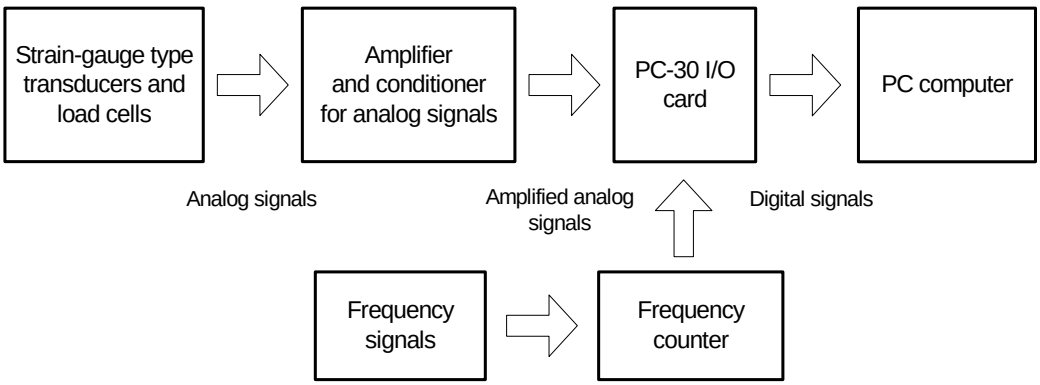

Figure 5.16. The flow chart for the data acquisition system.

Figure 5.17. The computer system in the cab ready for data logging.